A sub-tropical cirrus clouds climatology from Reunion Island (21°S, 55°E) lidar data set

Bertrand Cadet, Leah Goldfarb, Denis Faduilhe, Serge Baldy, V. Giraud, Philippe Keckhut, Anne Réchou

A sub-tropical cirrus clouds climatology from Reunion Island (21°S, 55°E) lidar data set

B. Cadet,[1] L. Goldfarb,[2] D. Faduilhe,[1] S. Baldy,[1] V. Giraud,[3] P. Keckhut,[2] and A. Réchou[1]

Received 26 September 2002; revised 5 November 2002; accepted 14 November 2002; published 11 February 2003.

[1] The aim of this work is to document cirrus characteristics using ground-based measurements. A climatology of sub-tropical cirrus clouds is presented from the analysis of the Rayleigh-Mie lidar data collected at the "Observatoire de Physique de l'Atmosphere de la Reunion" (OPAR) over the period 1996–2001. The lidar laser operates at 532 nm. This climatology is based on the analysis of upward laser beam over 533 nights corresponding to 1643 hours of lidar probing. In this sub-tropical zone, two main seasons prevail for cirrus clouds occurrence: an austral winter, from May to October, and an austral summer, from November to April. As expected, cirrus are present more frequently during the austral summer, 13% of measurements, than during the austral winter, 1%. Subvisible cirrus clouds, characterised by an optical thickness below 0.03, compose a significant fraction, 65%, of the total cirrus observations. *INDEX TERMS:* 1610 Global Change: Atmosphere (0315, 0325); 3309 Meteorology and Atmospheric Dynamics: Climatology (1620); 3374 Meteorology and Atmospheric Dynamics: Tropical meteorology; *KEYWORDS:* tropical cirrus, climatology, lidar. **Citation:** Cadet, B., L. Goldfarb, D. Faduilhe, S. Baldy, V. Giraud, P. Keckhut, and A. Réchou, A sub-tropical cirrus clouds climatology from Reunion Island (21°S, 55°E) lidar data set, *Geophys. Res. Lett.*, *30*(3), 1130, doi:10.1029/2002GL016342, 2003.

1. Introduction

[2] High-altitude clouds, like cirrus, have been identified as one important regulator of the radiance balance of the earth-atmosphere system [*Twomey*, 1991]. Through radiative effects, these clouds are likely to modulate climate system on all scales [*Ramanathan and Collins*, 1991; *Fu et al.*, 1995]. *Sassen and Cho* [1992] have proposed 0.03 threshold value for optical thickness at 694 nm to separate cirrus clouds in two types: visible cirrus (VC) and subvisible cirrus (SVC). *Wang et al.* [1996] showed that the radiative effects of SVC could be greater than 0.5 $W.m^{-2}$ in the tropics. Cirrus clouds properties are quite important for climate models [*Penner et al.*, 1999], particularly in the tropics where they have an occurrence frequency of ~20% [*Liou*, 1986]. From the Stratospheric Aerosol and Gas Experiment (SAGE) II observations, *Wang et al.* [1994] reported optically thin cirrus near the tropopause more than 50% of the total observational time. However, satellite cloud climatology derived from passive radiative measurements may underestimate the actual cirrus occurrence frequency. For example, *Wylie and Wang* [1997] showed that more cirrus were consistently detected when a more sensitive sensor with a larger field of view was used.

[3] Over the past two decades, laser and therefore lidar instrumentation has improved tremendously. Because of the precise ranging capabilities (good spatial and temporal resolution), the lidar technique is an attractive tool in observing cirrus clouds [*Evans et al.*, 1996; *Platt et al.*, 1987; *Sassen et al.*, 1990]. Its main limitation of ground based lidar measurements is that no information can be obtained when thick (i.e., opaque) low clouds occur.

[4] The OPAR is located in the Indian Ocean just above the tropic of Capricorn; it makes quasi-continuous measurements in the southern hemisphere where there is a dearth of cirrus measurements. We present in this study a sub-tropical cirrus climatology based on 6 years set lidar data recorded at the OPAR which constitutes the most temporally extensive lidar data base in the southern tropics.

[5] After a brief description of the OPAR lidar system and a short presentation of the data analysis method, we present two typical case studies. Our results are discussed with respect to the dominate air motions in this region.

2. Instrumentation and Data Analysis

[6] The Rayleigh-Mie lidar system has been operating at the OPAR (21°S, 55.5°E) since May 1994. A chronological description of the improvements made to this system have been detailed by *Baray et al.* [1999]. The Rayleigh-Mie lidar, in its present configuration, uses a Nd:Yag laser emitting at 532 nm and 1064 nm at 1 J and 1.75 J per pulse respectively. The light pulse duration is 7 ns and the repetition rate is 30 Hz. Backscattered photons are collected by three different systems of telescopes, allowing coverage of a wide vertical range, i.e., 1–90 km for non-polarized light and 1–30 km for polarized detection. The present work is based on the analysis of the 532 nm non-polarized backscatter signal with a vertical resolution of 150 m. The photons are collected by a 20 cm diameter telescope. Lidar data are recorded during nighttime, when no deep low altitudes clouds are present. A two-minutes integration time is used.

[7] We used a cirrus detection method similar to that described by *Goldfarb et al.* [2001] (GOL) for the northern hemisphere medium-latitudes site of Observatoire de Haute Provence (OHP) to facilitate future comparisons between sub-tropical and medium-latitudes cirrus climatologies.

[8] To determine the threshold for cirrus detection, first, the raw signal is corrected for the background and the altitude square dependence. Then, the Scattering Ratio (SR) is calculated by dividing the signal corrected for the

[1]CNRS/Laboratoire de Physique de l'Atmosphère, La Réunion, France.
[2]CNRS/Service d'aéronomie, Verrières-le-Buisson, France.
[3]Laboratoire d'Optique Atmosphérique, Villeneuve d'Ascq, France.

0094-8276/03/2002GL016342

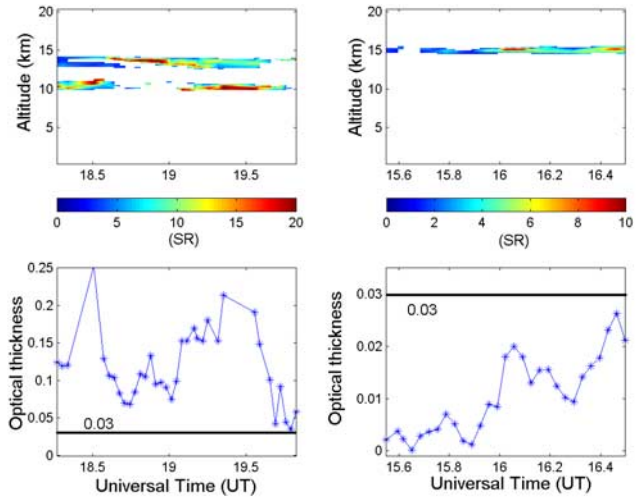

Figure 1. Case studies of multi-layer (a) and mono-layer (b) cirrus corresponding to 03/01/2001 and 09/09/98 respectively. The upper figures show, the SR as functions of time and altitude. SR values below cirrus detection threshold (t_{SR}, see text paragraph n°2 for definition) are not represented. The lower graphs show optical thickness as function of time. The horizontal line on the graphs represents the threshold value (0.03) between sub-visible cirrus and visible cirrus.

Mie + Rayleigh component by the corrected raw signal of Rayleigh contribution obtained by a forth degree polynomial fit. The result is:

$$SR = 1 + \beta_{Cirrus}/\beta_{Rayleigh} \quad (1)$$

where $\beta_{Rayleigh}$ and β_{Cirrus} are Rayleigh and Mie backscattering coefficients respectively.

[9] For the optical depth calculation, we used the next formula:

$$\tau_{Cirrus} = \int_{z_{base}}^{z_{top}} \alpha(z)dz = (LR)\sigma_{Rayleigh} \int_{z_{base}}^{z_{top}} n_{air}(z)(SR(z) - 1)dz \quad (2)$$

where α is the extinction coefficient, LR is the Lidar Ratio defined as: $LR = \alpha/\beta_{Cirrus}$ and n_{air} is the air density computed by the MSIS-E-90 atmosphere model [http://nssdc.gsfc.nasa.gov/space/model/models/msis.html].

[10] Cirrus occurrence frequency is obtained as the ratio of cirrus detection time versus the total measurement time.

[11] Cirrus detection is based on two simultaneous criteria being met: (1) the Scattering Ratio (SR) being greater than a threshold value (t_{SR}) defined as the sum of the nightly SR mean for the 23–25 km layer plus three times the SR standard deviation for this altitude range and (2) the cloud top layer is situated above (i.e., colder than) the altitude corresponding to −38°C altitude [*Sassen and Campbell*, 2001]. Temperatures were determined by radiosondes measurements launched from St Denis de la Réunion. Typically, the analogous altitude of the −38°C level is around 10 km. The reference layer (23–25 km) is higher and thicker (2 km) than the one used for OHP, since the tropopause is higher in the tropics (around 17 km, versus 12 km at OHP) and the OHP lidar vertical resolution is half the one used here.

[12] We use the same value for the lidar ratio (LR): 18.2 sr, value proposed by *Platt and Diley* [1984] to calculate the optical depth.

[13] Figures 1a and 1b show two nights where cirrus were detected. Cirrus are occasionally observed during the entire sampling time. In Plate 1a, a bi-layer cirrus cloud is observed. The lower layer is situated at 11 km and the upper at 14 km. Our criterion for distinct cirrus layers is a 300 m vertical separation (two times the native lidar vertical resolution). The total optical thickness varies from 0.03 to 0.25. In Plate 1b, a mono-layer cirrus is observed for entire observation time, located at 15 km. The maximum optical thickness is 0.025. These two illustrations show that partitioning clouds between two classes in using the threshold of the optical thickness is somewhat insufficient however it gives a useful preliminary distribution of cirrus characteristics.

3. Results

[14] During 1996–2001 period, the lidar system recorded 533 measurement nights representing a total of 1643 observation hours. On average, a measurement night corresponds to 3 hours, centred at 18 h (UT) for 76% of the measurements, and there are about 7.5 measurements nights per month since 1996. However, as seen in Figure 2, there are more nightly measurements during two periods: March to June and October to November. The reason for this is that there are fewer or no low level or deep convection clouds during these periods. The measurement distribution is affected by low cloud and deep convection only during the austral summer. The few data during July, August and October due to the reduction of personnel during these periods.

[15] Cirrus clouds occurrence is correlated with seasons (see Figure 2). The frequency peaks in December, with

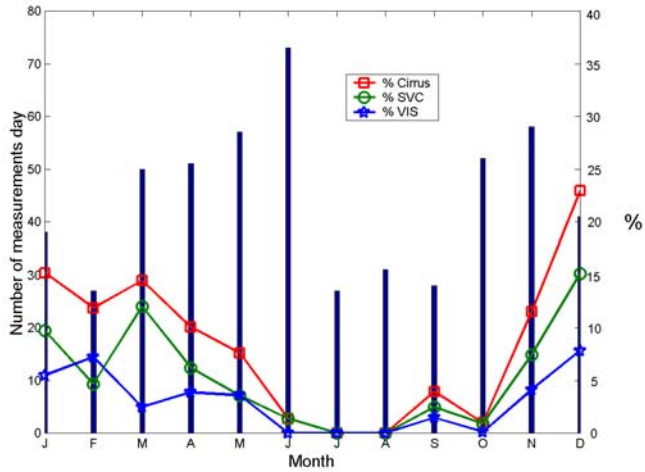

Figure 2. Cirrus occurrence frequency derived from lidar data over the 1996–2001 period. Total cirrus occurrence percentage (red), SVC percentage (green) and VC percentage (blue) as function of month. Vertical bars show the number of measurements.

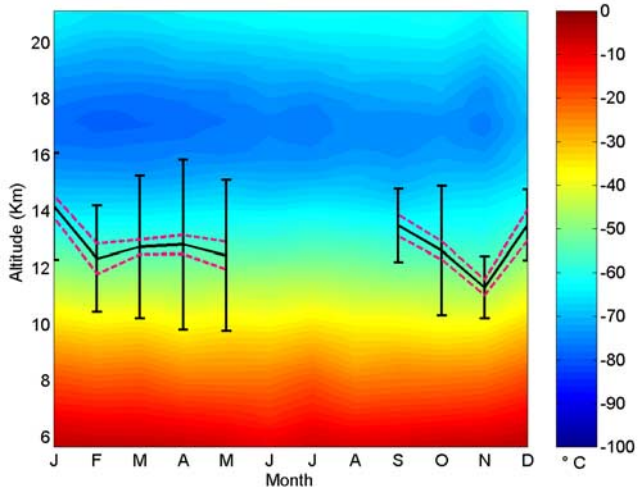

Figure 3. Evolution of the mean monthly temperature at the OPAR over the 1996–2001 period determined by radiosondes and mean monthly base, mid-cloud and top cirrus altitude with standard deviation for mid-cloud altitude.

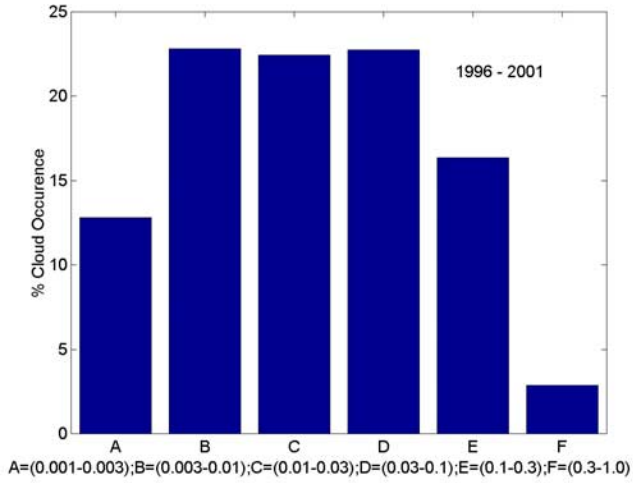

Figure 4. Histogram of cirrus optical thickness binned on log scale for the 1996–2001 period. Lettering along the abscissa corresponds to optical thickness intervals, which are given above. Categories A–C comprise the SVC component.

cirrus present more then 20% of the observational time; the minimum frequency is observed in July and August when no cirrus cloud are present during the 175 hours of measurements over the entire 6 year period. During the austral winter, cirrus frequency is less than 5% in contrast with the austral summer where the frequency is reaches 20%. This result is agreement to the results obtained by *Roumeau* [2001].

[16] The mean monthly mid-cloud cirrus altitude and 1 sigma intervals are represented in Figure 3. This altitude varies from 11 km to 14 km and reaches its maximum in January. Both SVC and VC show similar seasonal variations. The discrepancy between VC and SVC of mean monthly average altitude lays within the limits of the standard deviation of the mid-cloud mean altitude (12.9 ± 1.5 km). Not surprisingly, SVC are thinner (0.4 ± 0.4 km) than VC (1.4 ± 0.7 km). For the total observation period, cirrus clouds occurred without any other cloud system layer, 7% of the time. Of this 7%, 65% of the cirrus clouds were SVC. This percentage have to be associated with the value of LR equal to 18.2 sr, and the neglect of multiple scattering, which are the two principal sources of uncertainties to derive the optical depth in this study. In practice, the contribution of multiple scattering depends on the lidar measurement configuration and cloud optical depth but also on particle shape and size as the phase function will significantly differ from one type of crystal to another [*Chepfer et al.*, 1999]. Single wavelength lidar optical depth retrieval involves large uncertainty and SVC occurrence could hence be changed by a factor of two, as in GOL. For example, when we allow the LR to vary from 5 to 50 sr, the SVC percentage changes from 85 to 45% respectively.

[17] Yet, during February, where ITCZ is the closest, the frequency of VC (8%) is higher than SVC frequency (5%), for other months, SVC are more frequent than VC. Figure 4 shows the frequency of occurrence distribution of the optical depth. Categories B,C and D are the most frequent (optical thickness between 0.003–0.1).

[18] Of the 7% total cirrus occurrence, 81% are mono-layer, 16% bi-layer and 3% are tri-layer clouds.

4. Discussion and Conclusion

[19] The climatic context of the OPAR is typical of an oceanic site dominated by the southern Hadley cell circulation [*Baldy et al.*, 1996]. Two typical seasons can be distinguished depending on the position of the Inter Tropical Convergence Zone (ITCZ) with respect to the island. The austral winter (JJA) corresponds to a distant position of the ITCZ and a strong influence of the Hadley plus Walker cell that generates steady easterly trade winds at low altitudes (<3 km) and westerly trades above the trade wind inversion. The wind inversion blocks vertical exchange and thus, the relative humidity remains below 10% in the free troposphere most of the austral winter (Figure 5). During

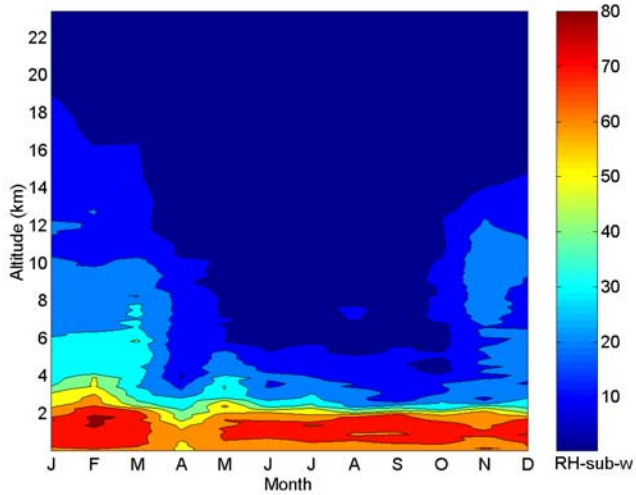

Figure 5. Evolution of the averaged monthly relative humidity (%) with respect to liquid water at the OPAR determined by radiosondes over 1996–2001 period.

austral summer (DJF), the ITCZ approaches the island and thus the trade wind influence is weak. The trade wind inversion is almost entirely vanishes during the summer. Water vapor from the Marine Boundary Layer is vented to the upper troposphere by intensive deep convection (and vice-versa in winter). The comparison of Figures 2 and 5 highlights the correlation between annual variation of water vapor in the atmosphere and cirrus clouds occurrence frequencies.

[20] Figure 3 shows a climatology of the atmosphere temperature over the OPAR. The Cold Point Temperature (CPT) can be used in the tropics to locate the tropopause. It is located around 17 km. Since convection penetrates more frequently at the upper levels [*Gettelman et al.*, 2002], the CPT is colder during the austral summer.

[21] We note the distinctive cirrus climatologies from OHP and OPAR. The difference in occurrence frequency is the most apparent difference. Mid-latitude cirrus are observed in 54% of the cases (GOL) all the year, while sub-tropical cirrus are present 7% of the time of observation and are depend on the season. Sub-tropical cirrus cloud heights occur 2.5 km higher than those at OHP. The proportion between SVC and VC are also different. However, the geometrical thickness of SVC and VC at the two stations are nearly the same.

[22] The frequency of cirrus occurrence is greatest during the austral summer at the OPAR. When no other tropospheric cloud system occurred, cirrus clouds with optical depth less than 0.03 dominates (65% of the cirrus clouds observed).

[23] This climatology is a first step to document cirrus by ground-based measurements in the important tropical zone. Detailed vertical and horizontal structures of cirrus clouds, including multi-layer analysis, particle size and shape, scale variability and heterogeneous chemical processes, are expected to be obtained from lidar systems able to penetrate thick cirrus. This system emits at two or more wavelengths and includes depolarization and Raman sub-systems. The Raman lidar provides precise information about the phase function of retro-diffusion (i.e., the inverse lidar ratio), then comparison with other climatology will be possible [*Sassen and Benson*, 2001]. As suggested by the two examples shown here (Figure 1), additional information will be a great help in portioning next climatology regarding the cirrus types formation.

[24] **Acknowledgments.** This work was supported by the "Laboratoire de Physique de l'Atmosphère" of Reunion Island University. The authors thankful M. Bessafi, for his help on radiosondes climatology and the technical team for their assistance. This work was funded by the INSU/PATOM and PNCA. B. Cadet is supported by a doctoral grant from the Region La Reunion.

References

Baldy, S., G. Ancellet, M. Bessafi, A. Badr, and D. Lan Sun Lunk, Field observations of the vertical distribution of tropospheric ozone at the island of Reunion (southern tropics), *J. Geophys. Res.*, *101*, 23,835–23,849, 1996.

Baray, J. L., J. Leveau, J. Porteneuve, G. Ancellet, P. Keckhut, F. Posny, and S. Baldy, Description and evaluation of the tropospheric ozone lidar implemented on an existing lidar in the southern subtropics, *Appl. Opt.*, *33*, 6808–6817, 1999.

Chepfer, H., J. Pelon, G. Brogniez, C. Flamant, V. Trouillet, and P. H. Flamant, Impact of cirrus cloud ice crystal shape and size on multiple scattering effects: Application to spaceborne and airborne backscatter lidar measurement during LITE mission and E LITE campaign, *Geophys. Res. Lett.*, *26*, 2203–2206, 1999.

Evans, W. E., E. J. Weigman, W. Viezee, and M. G. H. Ligda, Performance specifications for meteorological satellite lidar, NASA Report CR-760871, NTIS N66-2997, 174, 1996.

Fu, Q., S. K. Krueger, and K. N. Liou, Interactions between radiation and convection in simulated tropical cloud clusters, *J. Atmos. Sci.*, *52*, 1310–1328, 1995.

Gettelman, A., M. L. Salby, and F. Sassi, The distribution and influence of convection in the tropical tropopause region, *J. Geophys. Res.*, 4080, doi:10.1029/2001JD001048, 2002.

Goldfarb, L., P. Keckhut, M.-L. Chanin, and A. Hauchecorne, Cirrus climatological results from lidar measurements at OHP (44°N, 6°E), *Geophys. Res. Lett.*, *28*, 1687–1690, 2001.

Liou, K. N., Influence of cirrus clouds on weather and climate processes: A global perspective, *Mon. Weather Rev.*, *114*, 1167–1199, 1986.

Penner, J. E., D. H. Lister, D. J. Griggs, D. J. Dokken, and M. McFarland, *Aviation and the Global Atmopshere: Special Report of the Intergovernmental Panel on Climate Change*, Cambridge Univ. Press, New York, 1999.

Platt, C. M. R., and A. C. Diley, Determination of the cirrus particle single-scattering phase function from lidar and solar radiometric data, *Appl. Opt.*, *23*, 380–386, 1984.

Platt, C. M. R., J. C. Scott, and A. C. Diley, Remote sounding of high clouds, part VI, Optical properties of midlatitude and tropical cirrus, *J. Atmos. Sci.*, *44*, 729–747, 1987.

Ramanathan, V., and W. Collins, Thermodynamics regulation of ocean warming by cirrus clouds deduced from observations of the 1987 El-Niño, *Nature*, *351*, 27–32, 1991.

Roumeau, S., Les réactions hétérogènes dans la troposphère tropicale: Effet des aérosols carbonés et des cirrus sur l'ozone, Ph.D. thesis, Lab. de Phys. de l'Atmos., La Réunion, France, 2001.

Sassen, K., and S. Benson, A midlatitude cirrus cloud climatology from the Facility for Atmospheric Remote Sensing, part II, Microphysical properties derived from lidar depolarization, *J. Atmos. Sci.*, *58*, 2103–2112, 2001.

Sassen, K., and J. R. Campbell, A midlatitude cirrus cloud climatology from the Facility for Atmospheric Remote Sensing, part I, Macrophysical and synoptic properties, *J. Atmos. Sci.*, *58*, 481–496, 2001.

Sassen, K., and G. S. Cho, Subvisual-thin cirrus lidar dataset for satellite verification and climatological research, *J. Atmos. Meteorol.*, *31*, 1275–1285, 1992.

Sassen, K., C. J. Grund, J. D. Spinhirne, J. M. Alvarez, and M. J. Hardesty, The 27–28 October 1986 FIRE IFO cirrus case study: A five lidar overview of cloud structure and evolution, *Mon. Weather Rev.*, *118*, 2288–2312, 1990.

Twomey, S., Aerosols, clouds and radiation, *Atmos. Environ.*, *25*, 2435–2442, 1991.

Wang, P. H., M. P. McCormick, L. R. Poole, W. P. Chu, K. Yue, G. S. Kent, and K. M. Skeens, Tropical high cloud characteristics derived from SAGE II extinction measurements, *Atmos. Res.*, *34*, 53–83, 1994.

Wang, P. H., P. Minnis, M. P. McCormick, G. S. Kent, and K. M. Skeens, A 6-year climatology of cloud occurrences frequency from Stratospheric Aerosol and Gas Experiment II observations (1985–1990), *J. Geophys. Res.*, *101*, 29,407–29,429, 1996.

Wylie, D. P., and P. H. Wang, Comparison of cloud frequency data from the High-resolution Infrared Radiometer Sounder and the Stratospheric Aerosol and Gas Experiment II., *J. Geophys. Res.*, *102*, 29,893–29,900, 1997.

S. Baldy, B. Cadet, D. Faduilhe, and A. Réchou, CNRS/Laboratoire de Physique de l'Atmosphère, La Réunion 97400, France. (bcadet@univ-reunion.fr)

V. Giraud, Laboratoire d'Optique Atmosphérique, Villeneuve d'Ascq 59000, France.

L. Goldfarb and P. Keckhut, CNRS/Service d'aéronomie, Verrières-le-Buisson 91371, France.